WILEY | Hindawi

Research Article
Rheology and Thixotropy of Cement Pastes Containing Polyacrylamide

Zhenhua Su,[1] Chunxiao Li,[2] Guilin Jiang,[3] Jiajie Li,[4] Hao Lu (ORCID),[4] and Fenghui Guo[5]

[1]Changjiang River Scientific Research Institute, Huangpu Street No. 23, Wuhan, Hubei 430010, China
[2]Department of Transportation Engineering, Hebei University of Water Resources and Electric Engineering, Huanghe Road No. 49, Cangzhou, 061001 Hebei, China
[3]Yellow River Engineering Consulting Co., Ltd., Jinshui Road No. 109, Zhengzhou, Henan 450003, China
[4]College of Water Conservancy and Hydropower Engineering, Hohai University, Xikang Road No. 1, Nanjing, Jiangsu 210098, China
[5]Shenzhen Academy of Metrology and Quality Inspection, Tongfa Road No. 4, Nanshan District, Shenzhen, Guangdong 518000, China

Correspondence should be addressed to Hao Lu; 180402020005@hhu.edu.cn

In this article, the rheological and thixotropic properties of fresh cement pastes (fcps) with nonionic polyacrylamide (PAM) are investigated through the coaxial rotary method. The B-HB model is resorted to fit the shear stress versus shear rate diagram, from which the slurry plastic viscosity is particularly discussed. The results show that with the development of PAM, the plastic viscosity increases first, then decreases, and then increases again, exhibiting the "up-down-up" trend, which is consistent with the fcps fluidity. The adsorption, lubrication, and entanglement mechanisms of PAM are successfully used to interpret this phenomenon. Combined with the suspension density, the relationship among plastic viscosity, flowability, and density is successfully established follower via a multivariate linear regression method. The Durbin-Watson coefficient, variance inflation factor, μ significance, ρ significance, and R^2 are 2.122, 1.024, 0.014, 0.004, and 0.776, respectively, demonstrating the feasibility of fitting formula. Besides that, the PAM containing slurry which exhibits the explicit thixotropy is also found according to the appeared hysteresis curve during one shearing cycle. With the increase of PAM dosage, the thixotropic indexes including Th1 and Th2 decreased, until the PAM exceeded 0.5%-0.6% dosage, both of them yielded negative values. The phenomenon that the fcps final shear stress exceeds its initial value occurs.

1. Introduction

Polyacrylamide is a kind of linear high molecular polymer. Due to the amide group contained in its structural unit, it is easy for PAM to form hydrogen bonds, resulting in the good water solubility and high chemical activity [1]. Combined with grafting or cross-linking technology, various PAM modifications can be tailored for different industries, such as petroleum exploration, water treatment, textile, paper-making, mineral processing, medicine, and agriculture [2].

In the civil engineering field, polyacrylamides are commonly utilized as the viscosity modifying admixtures [3–5]. It can improve the yield stress of the cementing material while reducing the deformation of the material due to its own weight, which is the key of additive manufacturing concrete. Based on this property, PAM could be used in the field of shotcrete, single-coat plastering mortar or tile adhesives [6]. According to [7–9], the flocculation properties of fiber reinforced cement-based composites prepared by polyacrylamide could be appropriately tuned to ensure the casting process smoothly. Due to its ability of reducing bleeding, segregation, and significantly increasing the internal cohesion of the traditional concrete, PAM was always employed as the antiwashout admixture in underwater pouring, filling, or repair engineering [10–12]. In digital construction field, the fcps containing polyacrylamide were found to exhibit a

higher elastic modulus compared with cellulose ethers added suspension [2, 13]. Combined with its ability of limiting the deformation of deposited cement-based materials under their own weight, PAM is emerging as one of the most suitable viscosity modifying admixtures for 3D printing concrete. Despite so many engineering applications, compared with other chemical admixtures in the construction industry such as cellulose ethers [6, 13–23] or polysaccharide [24–28], the usage of polyacrylamide is mostly based on empirical data in industrial practice [2], and the exact acting mechanisms of PAM on cement slurry materials are still unclear.

Compared with traditional slump and water retention properties, rheological parameters have more essential properties in characterizing cement-based materials such as mixing, pumping and filling and can even affect the mechanical strength and durability of hardened materials [29, 30]. As the viscosity modifying admixtures, it is highly important to understand and adjust the rheological behavior of PAM-added systems accurately. Many models are used to characterize to try to characterizing the cement-based material rheological properties [31]. The Bingham model or the Herschel–Bulkley model is commonly proved effective for fitting rheology performances of concrete, mortar, or cement paste [9]. In [32], the AWC rheological parameters were performed with the Bingham model; thereby, their relationship with washout resistance was established. Nevertheless, a shear-thinning or thickening behavior always occurs when viscosity-modifying admixtures were added to cement-based materials in accordance with [33], which was against the linear correlations between shear stress and shear rate in Bingham model. In [14, 34], the Herschel-Bulkley model was proved more precisely to express the shear stress versus shear rate curves compared with traditional Bingham model, while the fitting of the Herschel-Bulkley model often fails to give the right yield stress, and the negative values were found in [9–11], which is obviously unrealistic.

Under this framework, the rheological properties of polyacrylamide-blended cement slurry were analyzed by using H-HB model and found that the change trend of the obtained plastic viscosity and macrofluidity under the different PAM content is highly correlated. The relationship between macrofluidity and microparameters of polyacrylamide slurry was established by multiple linear regression method. In addition, the PAM containing slurry that exhibits the explicit thixotropy is also found and confirmed according to the appeared hysteresis curve during one shearing cycle. With the increase of PAM dosage, the enhanced thixotropy are verified, which provided some guidance for pumping and construction of polymer-activated slurry.

2. Materials and Testing Methods

2.1. *Preparation of Fresh Cement Paste.* The generally acceptable Ordinary Portland Cement (P.O. 42.5R) conforming to GB175-2020 [35] was used in this study. The chemical composition of OPC was carried by the X-ray fluorescence method, as shown in Table 1. A Bettersize 2000 laser particle size distribution instrument was resorted to explore the OPC particle distribution, as shown in Figure 1. In this figure, the diagrams of frequency vs. diameter and frequency vs. cumulative mass content are illustrated with the black and red solid lines, respectively.

The chemical viscosities used is traditional commercial nonionic polyacrylamide. Its molecular weight is 10 million Daltons, and its molecular structure and physical picture are shown in Figure 2. Cement slurry ratio was processed with a fixed water cement ratio of 0.5, and polycarboxylic acid high-efficient water reducing agent was added with a 2.0% of cement weight [32, 36, 37]. PAM content was 0%, 0.1%, 0.2%, 0.3%, 0.4%, 0.5%, 0.6%, 0.7%, 0.8%, 0.9%, and 1.0% of cement weight, and the gradient contrast tests were conducted to obtain the more reliable results. The preparation process of cement slurry is carried out strictly in accordance with our previous tests [10].

2.2. *Rheological Testing.* The rheological properties of fcps were measured using an LVDT-1T coaxial rotary viscometer. The illustrations of rheological testing of fcps are shown in Figure 3. Based on the range of measured cement-water-ratio and the molecular weight of PAM, the selected geometry of the outer (Stator) and inner (Rotor) cylinders is shown in Figure 3(a). The diameter and height of rotor were 5.0 mm and 33.0 mm, respectively. The diameter and height of stator were 20.0 mm and 45.0 mm, respectively. The rheology testing was adopted immediately after mixing procedure, and the shear rate was set to increase from 2.5 s to 25 s in 10 steps with 15 s as the interval time. The specific schematic diagram of shear rate versus time is shown in Figure 3(b).

2.3. *Fluidity.* The fluidity was determined according to GB/T 2419-2005 [38] by dropping a jump table 25 times in 15 seconds. The average of the two perpendicular measurements was recorded as the simple extensibility, and the final fluidity result of a given proportion mixture was determined by averaging three independent samples.

2.4. *Density.* The fcps density was conducted strictly conforming to GB/T208-2014 [39]. After pouring the mixed cement slurry into a 100 ml measuring cylinder, the apparatus was vibrated to exhaust the entrapped air void, then scraped off the excess grout with a sharpener. The masses of the measuring cylinder and total mass of measuring cylinder and fcps were weighed separately. The density calculation formula is shown in

$$D = \frac{(m_2 - m_1)}{V}, \qquad (1)$$

where D is the density of fresh cement paste (%); m_1 refers to the measuring cylinder mass (g); m_2 refers to the total mass of measuring cylinder and fcps (g); V is the volume of measuring cylinder.

2.5. *Thixotropic Testing.* The fcps thixotropic testing was conducted with the coaxial rotary method similar to the rheology testing. The geometry and size of apparatus selected in

TABLE 1: Chemical composition of P.O. 42.5R cement.

Chemical constituents	CaO	SiO_2	Al_2O_3	Fe_2O_3	SO_3	MgO	K_2O	Na_2O	Minors
Content/%	66.65	17.88	6.35	3.72	2.66	0.61	0.85	0.12	1.16

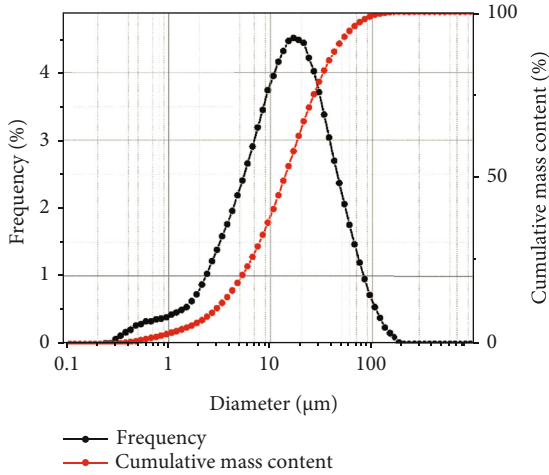Note: loss on ignition is 1.35%.

FIGURE 1: Particle size distribution of P.O. 42.5R cement.
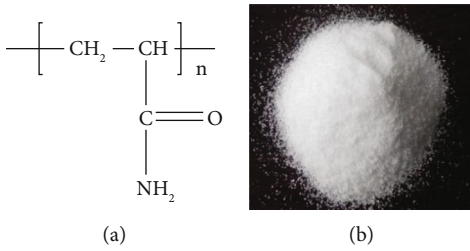

FIGURE 2: Monomer structure (a) and physical picture (b) of high molecular nonionic polyacrylamide.

this test were shown in Figure 3(a). The fcps thixotropic test protocol is displayed in Figure 4. The shear rate was set to increase from 2.5 s to 25 s in 10 steps at 15 s intervals firstly, and then, the shear rate was decreased from 25 s to 2.5 s in 10 steps at the same time interval.

3. Results and Analysis

3.1. Rheological Properties. The shear stress versus shear rate for fcps with different PAM dosages is displayed in Figure 5, where shear stresses are marked with different colors and shapes based on the PAM content. As the first observation, the acceleration of shear stress in PAM-added slurries decreased with increasing shear rate, indicating a decrease in material viscosity. The cement paste containing PAM exhibits pronounced shear-thinning behavior. This is because PAM belongs to the absorbable polymer, which could stick on the surface of cement particles through chelation or hydration bonds as the anchorage points [33]. Its

long-chain structure of polymers could simultaneously adsorb onto several cement grains and bridge them together [2], through the interaction between cement particles and polymer intermolecular as the connection nodes, resulting in the intertwining structures in the polymer system [7, 40]. With the progress of shear protocol, the network floc structure in fcps is gradually destroyed. Accompanied by linear alignment of the polymer long chains, the fcps resisting shear damage ability is subdued, leading to the shear-thinning behavior for PAM-added cement pastes.

With the increase of PAM content, the fcps shear-thinning behavior becomes less conspicuous. During shearing process, there not only exists slurry structural destruction; the inter-structure rebuilding also occurs in the form of PAM reabsorption and rewinding. This means that the structural damage and reconstruction of the cement slurry are constantly occurring during shearing process. When the PAM content is low, the slurry structure damage in the suspension system is dominant, and the material exhibits obvious shear-thinning behavior. With the growth of PAM content, the contact probability between PAM long-chain structures and cement particles increases. The structure reconstruction phenomenon is gradually enhanced, leading to the weakening of the shear-thinning behavior.

In order to study the rheological parameter characteristics of the slurry under the action of PAM polymer further, a new B-HB model is determined by taking advantage of the model of Bingham and Hershel-Bulkley while avoiding its shortcomings, as shown in Equation (2). For the first part of shear stress versus shear rate graph ($\gamma < 7.5\, s^{-1}$), Bingham model is used to get the yield stress and the plastic viscosity values. For the second part of shear stress versus shear rate graph ($\gamma > 7.5\, s^{-1}$), Herschel-Bulkley model is simulated through using the confirmed yield stress obtained in Bingham model to obtain the pseudoplastic index. The typical fitting schematics are shown in Figure 6, from which 0.2%, 0.5%, and 0.8% PAM are illustrated. In this paper, the plastic viscosity of the PAM addition system is analyzed emphatically, and its influence on the macroscopic flow properties of the material is studied, while the other parameters including yield stress and shear rate will be analyzed in our future study.

$$
\begin{cases}
\tau = \tau_0 + \mu\gamma & \gamma < 7.5\, s^{-1}, \\
\tau = \tau_0 + K\gamma^n & \gamma > 7.5\, s^{-1}.
\end{cases}
\tag{2}
$$

3.1.1. Plastic Viscosity. Figure 7 describes the plastic viscosity results of fcps with different PAM dosages, from which the plastic viscosities are shown in red circle dots in the left, and the corresponding dates are shown in the right. It is shown that, with the increase of PAM content, the plastic
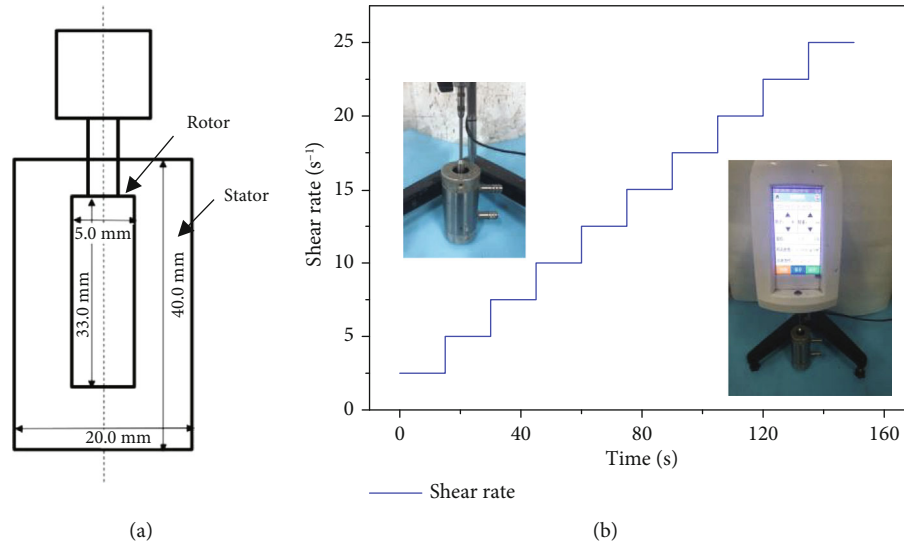
FIGURE 3: Diagrams of rheology test: (a) geometry of LVDT-1T coaxial rotary viscometer; (b) protocol of shear rate versus time.
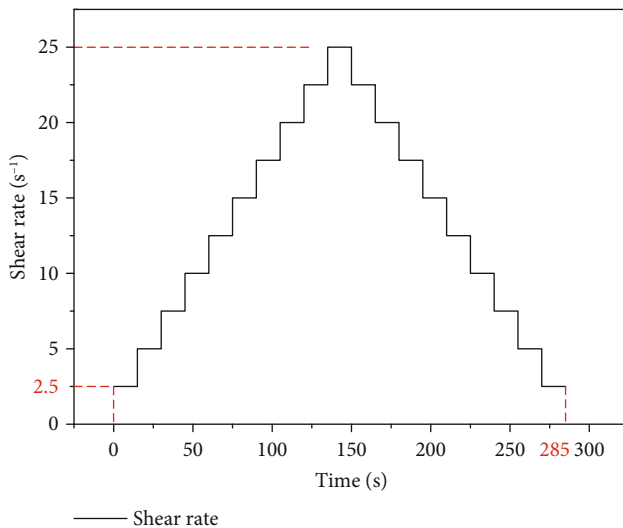

FIGURE 4: Schematic diagram of shear rate versus times in fcps thixotropy testing.

paper. In order to confirm the accuracy of rheological parameter results, the fluidity testing of the fcps with different PAM contents was further investigated.

3.1.2. Fluidity. The fluidity results of the cement slurry with different PAM contents were tested conforming to GB/T 2419-2005, and the results are shown in Figure 8. It is clearly demonstrated that, with the increase of PAM from 0.0% to 0.3%, the fcps flowabilities decrease sharply from 211.5 mm to 186.5 mm; then, the flowabilities increase from 186.5 mm to 200.0 mm as the PAM increase, from 0.3% to 0.7%; finally, the flowability values decrease again from 200.0 mm to 187.5 mm with continuous increase in PAM beyond 0.7% content, showing the "down-up-down" tendency. This trend highly corresponds with the plastic viscosity "up-down-up" tendency in B-HB model. This discovery, on the one hand, confirms the feasibility of B-HB model for simulating shear stress versus shear rate diagrams in PAM-added cement slurry system, and on the other hand, it also verifies that there are deficiencies in the understanding of the acting mechanisms of polymers on cement-based materials.

Combining the plastic viscosity and fluidity data, it can be found that the effects of PAM in cement can be attributed to three aspects, namely, adsorption (including particles and water molecules), lubrication, and entanglement. Due to the addition of polycarboxylate superplasticizer, cement particles in the suspension are dispersed uniformly, and the fcps plastic viscosity is low. When a small amount of PAM is added (PAM < 0.3%), PAM will be adsorbed on the surface of cement particles ascribed to the effect of hydrogen bonds and the chelation of alkali metals. Within this range, PAM mainly exhibits adsorption effect, i.e., adsorbing the water molecules in the suspension and alkali metals on the surface of cement particles. The cohesion of the suspension system is enhanced, and the plastic viscosity is increased. When 0.3% < PAM < 0.65%, the free water and particle surfaces

viscosity first increased (from 4.256 Ps·s to 9.237 Ps·s), then decreased (from 9.237 Ps·s to 3.480 Ps·s), and then increased (from 3.480 Ps·s to 5.147 Ps·s). Plastic viscosity is expressed as the flow resistance of the slurry internal structure, reflecting the cohesion of particle-to-particle phase, particle-to-liquid phase, and the continuous liquid phase under flow conditions. The results shown in Figure 7 indicate that, with the increasing of PAM dosage, the fcps flowability increases first, then decreases, and then decreases again. However, according to the upper established adsorption and entanglement mechanisms, fcps flow resistance will continue increase for the enhanced particle adsorption and structural entanglement with the increase of PAM dosage, leading to the rising values of the plastic viscosity. This is inconsistent with the "up-down-up" trend of plastic viscosity in this
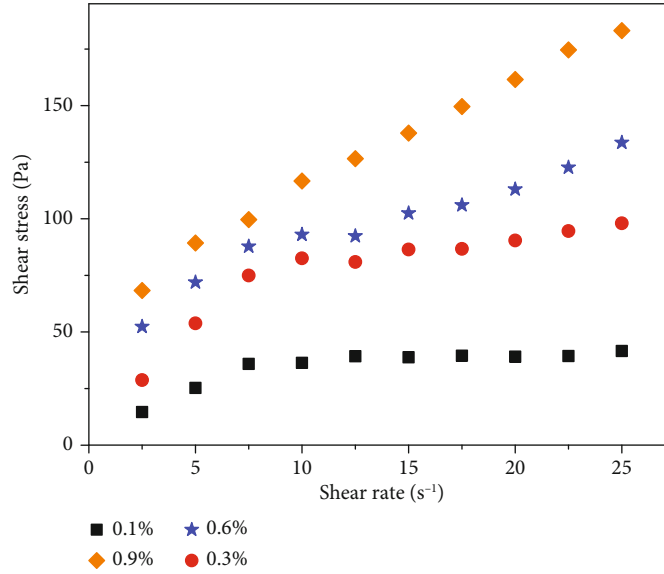
FIGURE 5: Shear stress versus shear rate for fcps with different PAM dosages.
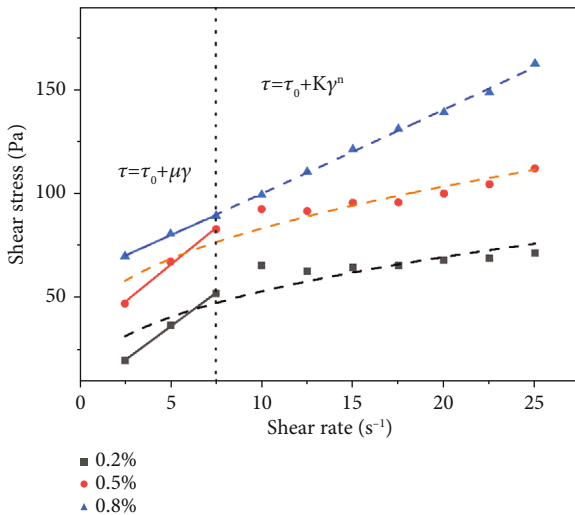

FIGURE 6: Fitting diagrams for fcps with 0.2%, 0.5%, and 0.8% dosages of PAM.

in the suspension system have been completely adsorbed, but the content of PAM is not high enough to form the entanglement structures at this time. The addition of PAM mainly existed in the form of pure solution, which is manifested as the lubricating effect between the cement particles. Within this range of PAM dosage, the cohesion of the suspension system is weakened by the existence of depletion attractive forces [41], and the plastic viscosity is reduced. When the PAM content in the cement slurry exceeds 0.65%, the entanglement effect between the polymer long-chain particles occurs and gradually dominates. The cohesion of the suspension system is enhanced again, leading to the increased plastic viscosity values. It should be noted that the above analysis of the action mechanism of different dosages of PAM in cement slurry is mainly based on rheological

and fluidity data. More relevant experiments are needed to perform to certify the accuracy of these mechanisms.

3.1.3. Relationships. Studying the rheological properties can predict and evaluate the pumping ability and flow stability capabilities of cement-based materials, yet rheometer components are sensitive, fragile, and expensive, making them unsuitable for construction sites. In contrast, traditional field test techniques such as slump expansion test and fluidity test have large human errors. Through establishing the functional relationship between flow rate and rheological parameters, the quantitative mixture rheological parameters can be obtained after the simple instrument testing. While avoiding cumbersome experimental operations, it can also achieve the purpose of predictably adjusting the rheological properties of the target material, meeting the requirements of on-site construction.

In 1993, De Larrard et al. [42] gave a method based on Bingham model and Herschel-Bulkley model for slump and yield stress of cement-based materials, respectively, as shown in Eq. (3) and Eq. (4) in Table 2. In Eq. (3), the plastic viscosity of the mixture is required to be lower than 300 Pa·s, and if it exceeds this value, the equation does not hold. As for Eq. (4), it is only applicable to cement-based materials whose yield stress is between 100 and 2000 Pa, and the calculated yield stress value below this range is documented smaller than the truth value. After that, Ferraris et al. [43] presented the relationship between plastic viscosity and density for the low-flow grout (slump value less than 260 mm) and provided a feasible solution for the conversion between rheological parameters and flow parameters. Based on the inherent performance parameters of the mixtures, Roussel et al. [44] established the relationship formula between the high flow slump and yield stress (slump value above 200 mm) after combining the Bingham and Herschel-Bulkley models, as shown in Eq. (7) in Table 2. The equation

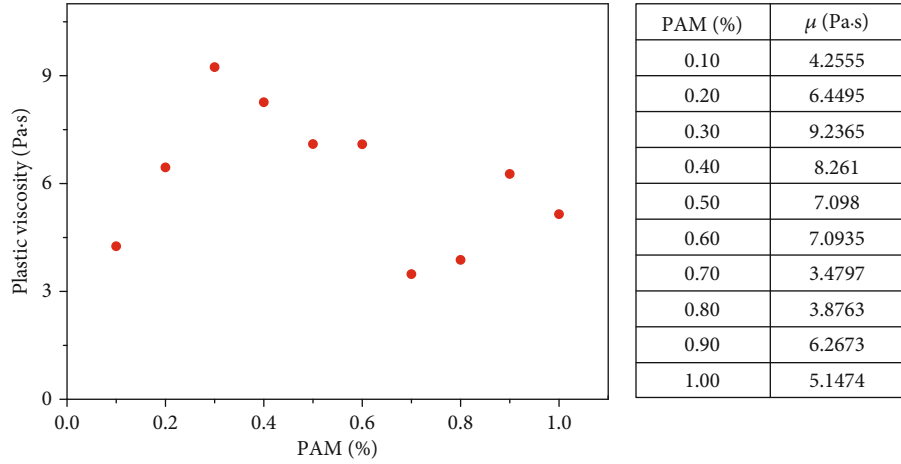| PAM (%)	μ (Pa·s)
0.10	4.2555
0.20	6.4495
0.30	9.2365
0.40	8.261
0.50	7.098
0.60	7.0935
0.70	3.4797
0.80	3.8763
0.90	6.2673
1.00	5.1474

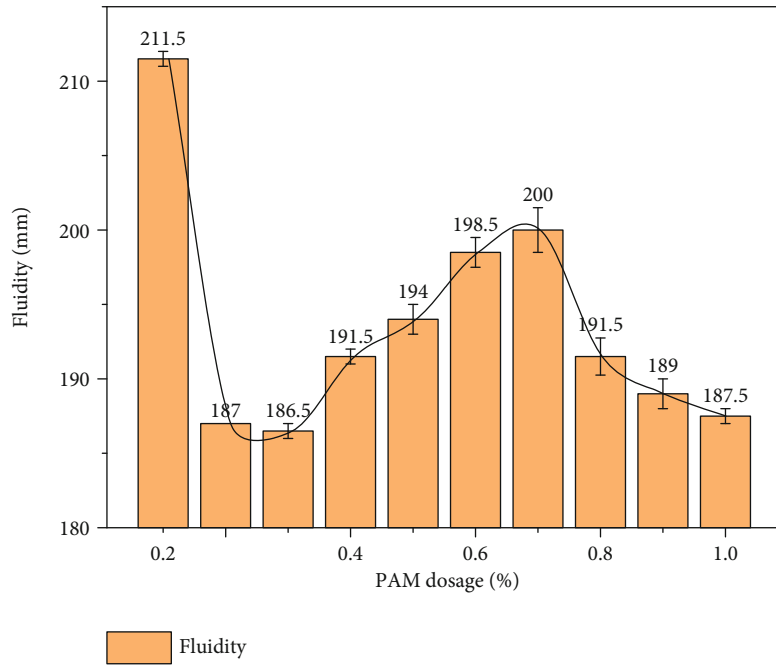FIGURE 7: Plastic viscosity results of fcps with different PAM dosages.

FIGURE 8: Fluidity results of fcps with different contents of PAM.

TABLE 2: Equations between flowability and rheological parameters.

Researchers	Equation	Number	Parameters	Model
De Larrard et al. [42]	$\tau_0 = \dfrac{\rho}{270}(300 - S)$	Eq. (3)	Yield stress; slump	Bingham
	$\tau_0 = \dfrac{\rho}{347}(300 - S) + 212$	Eq. (4)	Yield stress; slump	Herschel-Bulkley
Ferraris et al. [43]	$\mu = \rho T - 1.08(S - 175),\ 200\ \text{mm} < S < 260\ \text{mm}$	Eq. (5)	Yield stress; slump	—
	$\mu = 250\rho T,\ S < 200\ \text{m}$	Eq. (6)	Plastic viscosity; slump	—
Roussel et al. [44]	$\tau_0 = 1.747\rho V^2 r^{-5} - \lambda \dfrac{r^2}{V}$	Eq. (7)	Yield stress; slump	Bingham, Herschel-Bulkley

is not affected by the discrepancy of testing tools or materials, and it can directly transform the slump cone into a simple and effective rheological testing apparatus.

Nonetheless, few studies have been conducted on the relationship between rheological parameters and fluidity of polymers incorporated in fcps systems. In this paper, it has

TABLE 3: Density, plastic viscosity, and fluidity results of fcps with different PAM dosages.

PAM dosage (%)	Density (kg/m³)	Plastic viscosity (Pa·s)	Fluidity (mm)
0.1%	1749.00	4.26	21.15
0.2%	1722.60	6.45	19.70
0.3%	1688.38	9.24	18.65
0.4%	1670.75	8.26	19.15
0.5%	1685.82	7.10	19.40
0.6%	1657.11	7.09	19.85
0.7%	1650.46	3.48	20.00
0.8%	1631.73	3.88	19.15
0.9%	1611.62	6.27	18.90
1.0%	1607.75	5.15	18.75

TABLE 4: Model parameter results for multiple linear regression analysis.

Durbin-Watson coefficient	Variance inflation factor	μ significance	ρ significance	R^2
2.122	1.024	0.014	0.04	0.776
≈2.0	<5.0	<0.05	<0.05	—

been documented that the plastic viscosity of the mixture is consistent with the flowability. Combined with the inherent corresponding parameter, the relationship between plastic viscosity, fluidity, and density was successfully fitted by multiple linear regression method through SPSS software. The density, plastic viscosity, and fluidity results of fcps with different PAM dosages are shown in Table 3.

The SPSS fitting results and related model parameters of the multiple linear regression analysis are listed in Equation (3) and Table 4, and the reasonable ranges for each model parameter are listed in the last row of Table 4.

$$S = 0.385 - 0.231\mu + 0.012\rho, \qquad (3)$$

where S, μ, and ρ are the fluidity (mm), plastic viscosity (Pa·s), and density (kg/m³) of fresh cement paste, respectively.

The multiple linear regression requires the fitted parameter to meet the following two conditions: the parameters are independent of each other, i.e., the Durbin Watson coefficient is around 2.0; there is no multicollinearity between the variables, i.e., the variance inflation factor is less than 5.0. The results shown in Table 4 display that the Durbin Watson coefficient value and the variance inflation factor are 2.122 and 1.024, respectively. Both of which meet the requirements of the multiple linear regression, proving that the method is feasible to fit the relationship among the plastic viscosity, fluidity, and density. The significance analysis reveals that the significance of μ and ρ are 0.014 and 0.004, respectively, which are both less than 0.05, indicating that both density and plastic viscosity can effectively influence the fcps fluidity. Combined with the R-squared value of 0.776 in this equation, it can be concluded that Equation (3) can well express the relationship between the plastic viscosity, fluidity, and density of cement slurry under the incorporation of PAM.
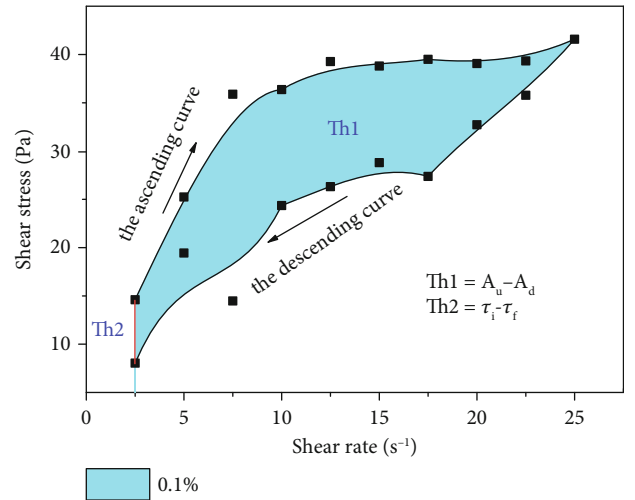

FIGURE 9: Diagrams of Th1 and Th2 values for fcps with 0.1%PAM.

3.2. Thixotropic Properties. Thixotropy refers to the property that fluid structures are damaged by shearing and gradually recover after shearing stops. During a shearing cycle, the flocculated structure formed by interparticle forces (such as van der Waals force and electrostatic force) breaks down into smaller flocs or individual particles with increasing shear rate, which is called the ascending curve. As the shear rate decreases, the material structure gradually recovers, and the decelerate of shear stress declines, which is called the descending curve. In this paper, the area of the hysteresis loop formed by the ascending and descending curves (Th1) and the difference between the initial and final shear stress (Th2) are used as indexes to represent the fcps thixotropy, as described in Figure 9.

From Figure 9, it can be seen that the fresh cement slurry after adding PAM has an obvious hysteresis curve,
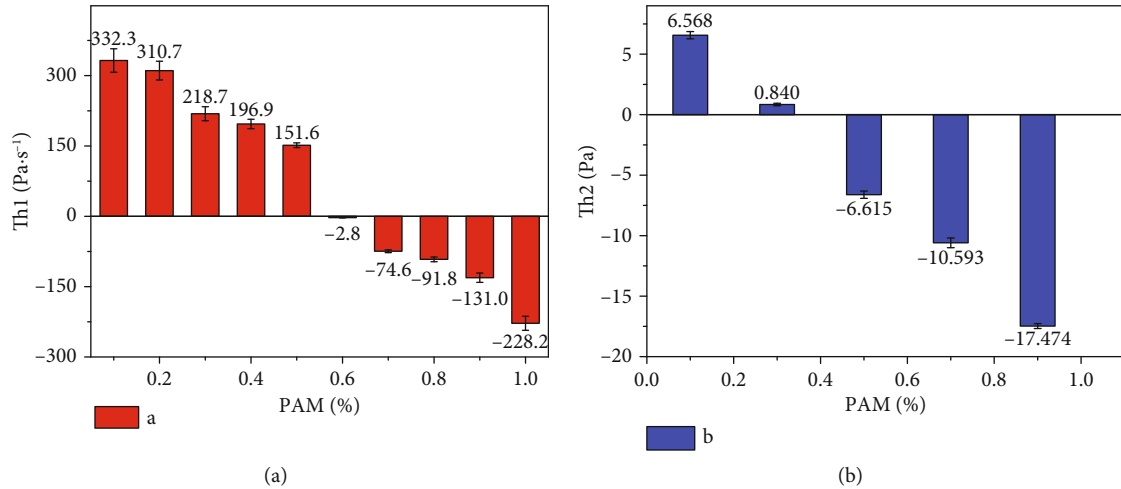
FIGURE 10: Th1 (a) and Th2 (b) results of fcps with different PAM dosages.

showing a thixotropy that does not exist in traditional cement slurry [45–47]. This can be explained by the fact that PAM can effectively enhance the cohesion ability between hydraulic particles, so that the larger shear destruction occurs during the shearing process of cement compared with the pure cement paste. In other words, the thixotropy of fcps is mainly attributed to the formation of network entanglement structures under the action of PAM.

The schematic diagrams of the specific Th1 and Th2 values changing with the PAM content are shown in Figure 10. It can be seen that the Th1 and Th2 values gradually decrease with the increase of PAM. The reduction in thixotropic indexes is related to the aforementioned structural remodeling. Due to the increase of PAM, the contact probability between cement particles and PAM increases. The suspension internal structure experiences the faster reabsorption and rewinding progress with the decreasing of the shear rate, resulting in the subdued final thixotropic properties. When the PAM content exceeds the range of 0.5%-0.6%, both of Th1 and Th2 show the negative values. This expounds that, with the continuous increase of PAM content, the recovery rate of fcps internal structure has exceeded the damage rate caused by shearing progress during the descending curve, and the final stress value is larger than the initial shear stress value.

4. Conclusion

This paper investigated the rheological and thixotropic properties of polyacrylamide in cement slurry. Through the experimental studies presented in this paper, the following conclusions can be reached:

(1) The B-HB model is used to fit the fcps rheology diagrams. The obtained plastic viscosity shows that with the increase of the PAM, its values increase first, then decrease, and increase again, showing the "up-down-up" tendency

(2) Based on the jump table results, the suspension exhibits the "down-up-down" tendency of fluidity values. The fcps fluidity corresponds to the plastic viscosity, verifying the feasibility of the B-HB model. This phenomenon can be rationally clarified by adsorption, lubrication, and entanglement mechanisms successively

(3) Combined with the density, the relationship between plastic viscosity, fluidity, and density is established through multiple linear regression analysis: $S = 0.385 - 0.231\mu + 0.012\rho$. The Durbin-Watson coefficient, variance inflation factor, μ significance, ρ significance, and R^2 are 2.122, 1.024, 0.014, 0.004, and 0.776, respectively, showing the effective fitting results

(4) The PAM-added fcps exhibits remarkable thixotropy according to the hysteresis curve in one shearing cycle. With the increase of PAM, the recovery rate of the internal structure of fcps accelerates, leading to the declined Th1 and Th2 values. When the PAM exceeds the range of 0.5%-0.6%, both thixotropic indexes yield the negative values, and the fcps final shear stress exceeds its initial value

Data Availability

Some or all data, models, or code that support the findings of this study are available from the corresponding author upon reasonable request.

Disclosure

The authors declare that the article described has not been published before, that it is not under consideration for publication anywhere else, and that its publication has been approved by all co-authors.

Conflicts of Interest

The authors declare that they have no known competing financial interests or personal relationships that could have appeared to influence the work reported in this paper.

Acknowledgments

References

[1] H. Li, D. Ni, L. Li, B. Dong, Q. Chen, and G. Linan, "Insight into the role of polyacrylamide polymer powder on the cracking in plastic period of cement mortar," *Construction and Building Materials*, vol. 260, p. 119914, 2020.

[2] H. Bessaies-Bey, R. Baumann, M. Schmitz, M. Radler, and N. Roussel, "Effect of polyacrylamide on rheology of fresh cement pastes," *Cement and Concrete Research*, vol. 76, pp. 98–106, 2015.

[3] F. Zhi, L. Jiang, M. Jin et al., "Inhibition effect and mechanism of polyacrylamide for steel corrosion in simulated concrete pore solution," *Construction and Building Materials*, vol. 259, p. 120425, 2020.

[4] Z. Sun and X. Qinwu, "Micromechanical analysis of polyacrylamide-modified concrete for improving strengths," *Materials Science and Engineering: A*, vol. 490, no. 1-2, pp. 181–192, 2008.

[5] A. Poursaee and C. M. Hansson, "Reinforcing steel passivation in mortar and pore solution," *Cement and Concrete Research*, vol. 37, no. 7, pp. 1127–1133, 2007.

[6] C. Brumaud, R. Baumann, M. Schmitz, M. Radler, and N. Roussel, "Cellulose ethers and yield stress of cement pastes," *Cement and Concrete Research*, vol. 55, pp. 14–21, 2014.

[7] C. Negro, L. M. Sánchez, E. Fuente, Á. Blanco, and J. Tijero, "Polyacrylamide induced flocculation of a cement suspension," *Chemical Engineering Science*, vol. 61, no. 8, pp. 2522–2532, 2006.

[8] C. Negro, L. M. Sánchez, H. Fuente, and A. Blanco, "Effects of flocculants and sizing agents on bending strength of fiber cement composites," *Cement and Concrete Research*, vol. 35, no. 11, pp. 2104–2109, 2005.

[9] C. Negro, A. Blanco, E. Fuente, L. M. Sánchez, and J. Tijero, "Influence of flocculant molecular weight and anionic charge on flocculation behaviour and on the manufacture of fibre cement composites by the Hatschek process," *Cement and Concrete Research*, vol. 35, no. 11, pp. 2095–2103, 2005.

[10] L. Hao, Z. Tian, M. Zhang, X. Sun, and Y. Ma, "Study on testing methods for water resistance of underwater cement paste," *Materials and Structures*, vol. 54, p. 180, 2021.

[11] E. Horszczaruk and P. Brzozowski, "Bond strength of underwater repair concretes under hydrostatic pressure," *Construction and Building Materials*, vol. 72, pp. 167–173, 2014.

[12] J. J. Assaad, Y. Daou, and K. H. Khayat, "Simulation of water pressure on washout of underwater concrete repair," *ACI Materials Journal*, vol. 106, no. 6, p. 529, 2009.

[13] C. Brumaud, H. Bessaies-Bey, C. Mohler et al., "Cellulose ethers and water retention," *Cement and Concrete Research*, vol. 53, pp. 176–184, 2013.

[14] C. Zhang, X. Kong, J. Yin, and F. Xiaochen, "Rheology of fresh cement pastes containing polymer nanoparticles," *Cement and Concrete Research*, vol. 144, p. 106419, 2021.

[15] C. Marliere, E. Mabrouk, M. Lamblet, and P. Coussot, "How water retention in porous media with cellulose ethers works," *Cement and Concrete Research*, vol. 42, no. 11, pp. 1501–1512, 2012.

[16] D. Bülichen, J. Kainz, and J. Plank, "Working mechanism of methyl hydroxyethyl cellulose (MHEC) as water retention agent," *Cement and Concrete Research*, vol. 42, no. 7, pp. 953–959, 2012.

[17] L. Patural, P. Marchal, A. Govin, P. Grosseau, B. Ruot, and O. Devès, "Cellulose ethers influence on water retention and consistency in cement-based mortars," *Cement and Concrete Research*, vol. 41, no. 1, pp. 46–55, 2011.

[18] J. Pourchez, B. Ruot, J. Debayle, E. Pourchez, and P. Grosseau, "Some aspects of cellulose ethers influence on water transport and porous structure of cement-based materials," *Cement and Concrete Research*, vol. 40, no. 2, pp. 242–252, 2010.

[19] L. Patural, P. Porion, H. Van Damme et al., "A pulsed field gradient and NMR imaging investigations of the water retention mechanism by cellulose ethers in mortars," *Cement and Concrete Research*, vol. 40, no. 9, pp. 1378–1385, 2010.

[20] M. Saric-Coric, K. H. Khayat, and A. Tagnit-Hamou, "Performance characteristics of cement grouts made with various combinations of high-range water reducer and cellulose-based viscosity modifier," *Cement and Concrete Research*, vol. 33, no. 12, pp. 1999–2008, 2003.

[21] D. Bülichen and J. Plank, "Role of colloidal polymer associates for the effectiveness of hydroxyethyl cellulose as a fluid loss control additive in oil well cement," *Journal of Applied Polymer Science*, vol. 126, no. S1, pp. E25–E34, 2012.

[22] M. Li, G. Shiyu, J. Jin, Y. Zheng, and D. Xie, "Research on the influence of polyanionic cellulose on the microstructure and properties of oil well cement," *Construction and Building Materials*, vol. 259, p. 119841, 2020.

[23] S. Tong, X. Kong, H. Tian, and D. Wang, "Effects of comb-like PCE and linear copolymers on workability and early hydration of a calcium sulfoaluminate belite cement," *Cement and Concrete Research*, vol. 123, p. 105801, 2019.

[24] T. Poinot, M.-C. Bartholin, A. Govin, and P. Grosseau, "Influence of the polysaccharide addition method on the properties of fresh mortars," *Cement and Concrete Research*, vol. 70, pp. 50–59, 2015.

[25] E. Ibrahim, M. Isik, and H. Ozkul, "Utilization of polysaccharides as viscosity modifying agent in self-compacting concrete," *Construction and Building Materials*, vol. 72, pp. 239–247, 2014.

[26] M. Sonebi, "Rheological properties of grouts with viscosity modifying agents as diutan gum and welan gum incorporating pulverised fly ash," *Cement and Concrete Research*, vol. 36, no. 9, pp. 1609–1618, 2006.

[27] Y. Yan, K. L. Scrivener, C. Yu, A. Ouzia, and J. Liu, "Effect of a novel starch-based temperature rise inhibitor on cement hydration and microstructure development: The second peak study," *Cement and Concrete Research*, vol. 141, p. 106325, 2021.

[28] M. C. G. Juenger and H. M. Jennings, "New insights into the effects of sugar on the hydration and microstructure of cement pastes," *Cement and concrete research*, vol. 32, no. 3, pp. 393–399, 2002.

[29] N. Roussel, *Understanding the Rheology of Concrete*, Woodhead Publishing, France, 2012.

[30] S. E. Chidiac, O. Maadani, A. G. Razaqpua, and N. P. Mailvaganam, "Correlation of rheological properties to durability and strength of hardened concrete," *Journal of Materials in Civil Engineering*, vol. 15, no. 4, pp. 391–399, 2003.

[31] A. Yahia and K. H. Khayat, "Applicability of rheological models to high-performance grouts containing supplementary cementitious materials and viscosity enhancing admixture," *Materials and Structures*, vol. 36, no. 6, pp. 402–412, 2003.

[32] K. H. Khayat and J. Assaad, "Relationship between washout resistance and rheological properties of high-performance underwater concrete," *Materials Journal*, vol. 100, no. 3, pp. 185–193, 2003.

[33] Kamal Henri Khayat, "Rheological properties of ultra-high-performance concrete – an overview," *Cement and Concrete Research*, vol. 124, p. 105828, 2019.

[34] X. Wenbin, M. Tian, and Q. Li, "Time-dependent rheological properties and mechanical performance of fresh cemented tailings backfill containing flocculants," *Minerals Engineering*, vol. 145, p. 106064, 2020.

[35] Common Porland Cement (GB175-2020), *China Standardization Administration of the People's Republic of China (in Chinese)*, 2020.

[36] M. Sonebi and K. H. Khayat, "Effect of mixture composition on relative strength of highly flowable underwater concrete," *Materials Journal*, vol. 98, no. 3, pp. 233–239, 2001.

[37] K. H. Khayat, "Effects of antiwashout admixtures on properties of hardened concrete," *ACI Materials Journal*, pp. 134–146, 1996.

[38] GB/T 2419-2005, "Test method for fluidity of cement mortar," in *The Standardization Administration of China*, Beijing, China, 2005.

[39] "Test method for determinging cement density (GB/T 208-2014), China," *Standardization Administration of the People's Republic of China (in Chinese)*, vol. 2014.

[40] D. Hou, X. Jianyu, Y. Zhang, and G. Sun, "Insights into the molecular structure and reinforcement mechanism of the hydrogel-cement nanocomposite: an experimental and molecular dynamics study," *Composites Part B: Engineering*, vol. 177, p. 107421, 2019.

[41] H. Bessaies-Bey, M. Palacios, E. Pustovgar et al., "Non-adsorbing polymers and yield stress of cement paste: effect of depletion forces," *Cement and Concrete Research*, vol. 111, pp. 209–217, 2018.

[42] F. De Larrard, J. Szitcar, and C. Hu, *Special Concretes-Workability and Mixing*, P. J. M. Bartos, Ed., CRC Press-France, 1993.

[43] "Testing and modelling of fresh concrete rheology, the United States," *National Institute of Standards and Technology Internal Report*, 1998.

[44] N. Roussel, C. Stefani, and R. Leroy, "From mini-cone test to Abrams cone test: measurement of cement-based materials yield stress using slump tests," *Cement and Concrete Research*, vol. 35, no. 5, pp. 817–822, 2005.

[45] M. Chen, B. Liu, L. Li et al., "Rheological parameters, thixotropy and creep of 3D-printed calcium sulfoaluminate cement composites modified by bentonite," *Composites Part B: Engineering*, vol. 186, p. 107821, 2020.

[46] W. Zhong, J. Ouyang, D. Yang, X. Wang, Z. Guo, and K. Hu, "Effect of the in situ leaching solution of ion-absorbed rare earth on the mechanical behavior of basement rock," *Journal of Rock Mechanics and Geotechnical Engineering*, 2021.

[47] W. Hao, G. Zhao, and S. Ma, "Failure behavior of horseshoe-shaped tunnel in hard rock under high stress: phenomenon and mechanisms," *Transactions of Nonferrous Metals Society of China*, vol. 32, no. 2, pp. 639–656, 2022.